

Dear authors,

Thank you for carefully revising the manuscript according to the comments from two referees and from myself. The manuscript has been significantly improved and augmented. I think it provides interesting results to the atmospheric science community, especially with the addenda of sections 4.4 and 5. Since I asked for these addenda, I didn't send the revised manuscript back to the referees but did the 2nd review myself. Please see the specific comments and questions below and a few edits in the annotated manuscript.

Specific comments

GNSS processing: did you include GPS and observations from other systems? I couldn't find this information.

P4L131-134 : I guess you refer to the monthly statistics of ZTD and/or gradient differences (GPS – ERAI) ? This is a post-processing QC, so maybe it should not be mentioned in this section.

P4L147-158 : on the impact of 3-day combination vs. 1-day solution. This discussion is useful and answers a comment from 1st referee. However, I think Figure 2 should not be presented in this paper since it is from a different analysis centre. Please removed the figure and revise the text.

P6L225-226: Explain why the improvement is smaller for GO4.

P7L255-258: Why do you think the residuals are dominated by errors due to modelling of tropospheric parameters, and particularly the wet contribution?

P7L266-278: this discussion calls for more careful interpretation. I think there is no evidence that the bias is due to ERA-Interim data (L268). If this statement is based on the GNSS comparison, assuming GNSS is the reference, it should be proved first that GNSS can sense the absolute ZTDs with an accuracy better than 1.8 mm. The fact that a similar bias was observed with other GNSS software doesn't mean that the bias is not in the GNSS estimates (L269). It just indicates that the bias is not software-dependent. A common bias might be due to the use of the same satellite products, similar tropospheric model, the regional-scale network...

P7L274-278: These comments don't add something to this study.

P8L299-301 and Figure 6-7: It is not clear what the statistics mean exactly. Are all values put together or is there an order of computation with respect to time and stations? It should be clearly explained how the means, standard deviations and error-bars are computed. The error bars seem very large for standard errors (by definition representing the uncertainty of the computed value). My interpretation is that the mean bias and standard of deviation of ZTD differences are first computed for each station and each month, and then mean and standard of deviation of these values are computed and the means are plotted +/- 1- standard of deviation. This would mean that the error bars represent the 1-sigma range (or dispersion) of values over the ensemble of stations. This is something different from standard error and uncertainty.

Table 4: similar comment: explain how the mean +/- dispersion (?) values are computed.

P9L333-342 and L350-359: recombine these two paragraphs

General comments on Section 4.4:

- The comparisons presented in this section are relevant and the discussion is well organised, comparison after comparison, referring to Table 5 and the different figures.
- I suggest to go in the same order for each discussion, commenting first on the median and min/max values in Table 5, and then on the latitudinal and height variations, and finally on the time evolution.
- Since latitudinal variations are more relevant I suggest switching the order of Figure 8 and 9.
- There is in general no trend with height, except in GO1-GO0. However, the increased scatter at low heights might be mentioned (for all comparisons). Is there an explanation?
- Add median values (e.g. as solid line) on the plots in Figure 10. It is important to check if there are drifts over time.
- The maps provided in the supplementary material could be included in the manuscript and referred to in complement to the latitudinal and height variations (Fig. 8, 9).
- Instead, it would be appropriate to provide in the supplementary material a table or a text file with the results plotted in the maps and in Figure 9 (overall statistics by station, including latitude, longitude and station height).
- Use the term 'bias' throughout the text to be consistent with the figures and tables, instead of using sometimes 'systematic errors'.

Specific comments on Section 4.4

P10L383: I think the differential performance of GMF/GPT and VMF1 has been studied and published by Boehm et al., and the increased errors of GMF/GPT at higher latitudes is a known issue. Please check the literature and provide adequate comments and references on this issue.

P10L386: Effect is attributed to more low-elevation observations over time. It would be nice that you document the time evolution of the number of (low-elevation) observations to provide evidence for this effect. Since you processed the data you have all the necessary information. This is usually not possible to check for end users (e.g. from the meteorological community).

L395: conclude on the sensitivity of results on the cutoff angle.

L398: could the degradation prior to 2002 be due to a change in the processing method or in pressure data used to compute the atmospheric loading?

L401-403: the scatter in bias and std is the largest for this comparison (GO4-GO1). Since coordinates are fixed, I guess that uncorrected atmospheric loading in GO1 solution is compensated by ZTD biases. Is this what you mean?

L414: why would the asymmetry be more imperfectly modelled with one tropospheric gradient every 6 hours rather than one per 24 hours? It seems more logical that the model with more parameters is better.

General comments on Section 5

The goal here is to assess the impact of variants on trend estimates. Though a detailed analysis of trend estimates is out of scope of this paper, the results shown in Figure 11 should be more

thoroughly commented and maybe completed with mean values per variant, or differences of variants like in section 4.4. It seems to me that GO0 and GO1 yield very similar trends, which means that the mapping function and ZHD don't have a strong impact. Cutoff angle has an impact (as previously shown by Ning and Elgered, 2012). Variants GO4, GO5, and GO6 are very similar, but not consistent with GO1, which means that non-tidal atmospheric loading has a significant impact.

It would be very valuable if trends were computed for all stations and all variants and the mean values and std summarized in a Table per variant. Conclusions could thus be more statistically significant. Then I would also suggest to provide the trend and uncertainty estimates per station as a supplement for further intercomparison with similar publications in the COST Special Issue (Baldisz et al., AMT-9-4861-2016, Klos et al. AMT-2016-385).

Specific comments on Section 5

P11L419 : add a reference to Eq (2), e.g. Weatherhead et al., 1998 ; Bock et al., 2014

Weatherhead, E. C., et al. (1998), Factors affecting the detection of trends: Statistical considerations and applications to environmental data, *J. Geophys. Res.*, 103(D14), 17,149–17,161, doi:10.1029/98JD00995.

P11L423 : seasonal, sub-seasonal and high-frequencies => be more specific: e.g., annual and 2nd, 3rd... harmonics.

P11L427 : Note that the noise is assumed white and thus the formal errors of the trend estimates are underestimated by a factor 2-4 (Nilsson and Elgered, 2008 ; Klos et al. AMT-2016-385).

Nilsson, T., and G. Elgered (2008), Long-term trends in the atmospheric water vapor content estimated from ground-based GPS data, *J. Geophys. Res.*, 113, D19101, doi:10.1029/2008JD010110.

P11L428-429 : The impact of cutoff angle was already reported by Ning and Elgered (2012).

Ning, T., and G. Elgered (2012), Trends in the atmospheric water vapor content from ground-based GPS: The impact of the elevation cutoff angle, *IEEE J. Sel. Top. Appl. Earth Obs. Remote Sens.*, 5, 744–751, doi:10.1109/JSTARS.2012.2191392.

P11L428-429 : differences don't reach 1 or 0.5 mm/year, please correct.

Section 6 : suggest to move it after section 3 (so change numbering of subsequent sections) as the focus is more on observation level and data processing.

P11L431-432 : is this web interface available to the scientific community ?

P11L454 : could you add the ZTD difference series on Figure 12 ?

At the end of section 6 it is not clear if the problematic stations/periods were removed from the dataset analysed in previous sections?

Table 4: 0.43 is repeated in the last column

Tropospheric products of the 2nd European GNSS reprocessing (1996-2014)

Jan Dousa, Pavel Vaclavovic, Michal Elias

NTIS - New Technologies for the Information Society, Geodetic Observatory Pecný, RIGTC
250 66 Zdíby, Czech Republic

Correspondence to: J. Douša (jan.dousa@pecny.cz)

Abstract

In this paper, we present results of the 2nd reprocessing of all data from 1996 to 2014 from all stations in the European GNSS permanent network as performed at the Geodetic Observatory Pecný (GOP). While the original goal of this research was to ultimately contribute to new realization of the European terrestrial reference system, we also aim to provide a new set of GNSS tropospheric parameter time series with possible applications to climate research. To achieve these goals, we improved a strategy to guarantee the continuity of these tropospheric parameters and we prepared several variants of troposphere modelling. We then assessed all solutions in terms of the repeatability of coordinates as an internal evaluation of applied models and strategies, and in terms of zenith tropospheric delays (ZTD) and horizontal gradients with those of ERA-Interim numerical weather model (NWM) reanalysis. When compared to the GOP Repro1 solution, the results of the GOP Repro2 yielded improvements of approximately 50% and 25% in the repeatability of the horizontal and vertical components, respectively, and of approximately 9% in tropospheric parameters. Vertical repeatability was reduced from 4.14 mm to 3.73 mm when using the VMF1 mapping function, a priori ZHD, and non-tidal atmospheric loading corrections from actual weather data. Raising the elevation angle cut-off from 3° to 7° and then to 10° increased RMS from coordinates' repeatability, which was then confirmed by independently comparing GNSS tropospheric parameters with the NWM reanalysis. The assessment of tropospheric horizontal gradients with respect to the ERA-Interim revealed a strong sensitivity of estimated gradients to the quality of GNSS antenna tracking performance. This impact was demonstrated at the Mallorca station, where gradients systematically grew up to 5 mm during the period between 2003 and 2008, before this behaviour disappeared when the antenna at the station was changed.

Keywords: GPS, reprocessing, zenith tropospheric delay, tropospheric horizontal gradients, coordinate time series, reference frame

1 Introduction

The US Global Positioning System (GPS) became operational in 1995 as the first Global Navigation Satellite System (GNSS). Since that time, this technology has been transformed into a fundamental technique for positioning and navigation in everyday life. Hundreds of GPS permanent stations have been deployed for scientific purposes throughout Europe and the world, and the first stations have collected GPS data for approximately the last two decades. In 1994, a science-driven global network of continuously operating GPS stations was established by the International GNSS Service, IGS (<http://www.igs.org>) of the International Association of Geodesy (IAG) to support the determination of precise GPS/GNSS orbits and, clocks and earth rotation parameters, which are necessary for obtaining high-accuracy GNSS analyses for scientific applications. A similar network, but regional in its

scope, was also organized by the IAG Reference Frame Sub-Commission for Europe (EUREF) in 1996, which was called the EUREF Permanent Network (EPN), <http://epncb.oma.be> (Bruyninx et al. 2012). Although its primary purpose was to maintain the European Terrestrial Reference System (ETRS), the EPN also attempted to develop a pan-European infrastructure for scientific projects and co-operations (Ihde et al. 2014). Since 1996, the EPN has grown to include approximately 300 operating stations, which are regularly distributed throughout Europe and its surrounding areas. Today, EPN data are routinely analysed by 18 EUREF analysis centres.

Throughout the past two decades, GPS data analyses of both global and regional networks have been affected by various changes in processing strategy and updates of precise models and products, reference frames and software packages. To reduce discontinuities in products, particularly within coordinate time series, homogeneous reprocessing was initiated by the IGS and EUREF on a global and regional scale, respectively. To exploit the improvements in these IGS global products, the 2nd European reprocessing was performed in 2015-2016, with the ultimate goal of providing a newly realized ETRS.

Currently, station coordinate parameter time series from reprocessed solutions are mainly used in the solid earth sciences as well as to maintain global and regional terrestrial reference systems. Additionally, from an analytical perspective, the long-term series of estimated parameters and their residuals are useful for assessing the performances of applied models and strategies over a given period. Moreover, tropospheric parameters derived from this GNSS reanalysis could be useful for climate research (Yuan et al., 1993), due to their high temporal resolution and unrivalled relative accuracy for sensing water vapour when compared to other techniques, such as radio sounding, water vapour radiometers, and radio occultation (Ning, 2012). In this context, the GNSS Zenith Tropospheric Delay (ZTD) represents a site-specific parameter characterizing the total signal path delay in the zenith due to both dry (hydrostatic) and wet contributions of the neutral atmosphere, the latter of which is known to be proportional to precipitable water (Bevis et al. 1994).

With the 2nd EUREF reprocessing, the secondary goal of the GOP was to support the activity of Working Group 3 of the COST Action ES1206 (<http://gnss4swec.knmi.nl>), which addresses the evaluation of existing and future GNSS tropospheric products, and assesses their potential uses in climate research. For this purpose, GOP provided several solution variants, with a special focus on optimal tropospheric estimates, including VMF1 vs. GMF mapping functions, the use of different elevation cut-off angles, and estimates of tropospheric horizontal gradients using different time resolutions. Additionally, in order to enhance tropospheric outputs, we improved the processing strategy in a variety of ways compared to the GOP Repro1 solutions (Douša and Václavovic, 2012): 1) by combining tropospheric parameters in midnights and across GPS week breaks, 2) by checking weekly coordinates before their substitutions in order to estimate tropospheric parameters, and 3) by filtering out problematic stations by checking the consistency of daily coordinates. The results of this GOP reprocessing, including all available variants, were assessed using internal evaluations of applied models and strategy settings, and external validations with independent tropospheric parameters derived from numerical weather reanalyses.

In Section 2, we describe the processing strategy used in the 2nd GOP reanalysis of the EUREF permanent network. In Section 3, we describe the approach developed to guarantee continuity of estimated tropospheric parameters at midnights as well as between different GPS weeks. In Section 4,

we present the results of internal and external evaluations of GOP solution variants and processing models. In Section 5, we present the relationship between mean tropospheric horizontal gradients and the quality of low-elevation GNSS tracking, which requires a more detailed study in the future. In the last section, we conclude our findings and suggest avenues of future research.

2 GOP processing strategy and solution variants

The EUREF GOP analysis centre was established in 1997, and contributed to operational EUREF analyses until 2013 by providing final, rapid, and near real-time solutions. Recently, GOP changed its contributions to that of a long-term homogeneous reprocessing of all data from the EPN historical archive. The GOP solution of the 1st EUREF reanalysis (Repro1) (Völksen, 2011) comprised the processing of a sub-network of 70 EPN stations during the period of 1996-2008. In 2011, for the first time, GOP reprocessed the entire EPN network (spanning a period of 1996-2010) in order to validate the European reference frame and to provide the first homogeneous time series of tropospheric parameters for all EPN stations (Douša and Václavovic, 2012).

In the 2nd EUREF reprocessing (Repro2), GOP analysed data obtained from the entire EPN network from a period of 1996-2014 using the Bernese GNSS Software V5.2 (Dach et al., 2015). The GOP strategy relies on a network approach utilizing double-difference observations. Only GPS data from the EPN stations were included according to official validity intervals provided by the EPN central Bureau (<http://epncb.oma.be>). Two products were derived from the reprocessing campaign in order to contribute to a combination at the EUREF level performed by the coordinator of analysis centres and the coordinator of troposphere products: 1) site coordinates and corresponding variance-covariance information in daily and weekly SINEX files and 2) site tropospheric parameters in daily Tro-SINEX files.

This GOP processing was clustered into eight subnetworks (Figure 1) and then stacked into daily network solutions with pre-eliminated integer phase ambiguities when ensuring strong ties to IGS08 reference frame. This strategy introduced state-of-the-art models (IERS Conventions, 2010) that are recommended as standards for highly accurate GNSS analyses, particularly for the maintenance of the reference frame. Additionally, the use of precise orbits obtained from the 2nd CODE global reprocessing (Dach et al., 2014) guaranteed complete consistency between all models on both the provider and user sides. Characteristics of this GOP data reprocessing strategy and their models are summarized in Table 1. Additionally, seven processing variants were performed during the GOP Repro2 analysis for studying selected models or settings: a) applying blind GMF (Böhm et al., 2006a) vs. actual VMF1 (Böhm et al., 2006b) tropospheric mapping functions, b) increasing the temporal resolution of tropospheric linear horizontal gradients in the north and east directions, c) using a different elevation angle cut-off, d) modelling atmospheric loading effects, and e) modelling higher-order ionospheric effects. Table 2 summarizes the settings and models of solution variants selected for generating coordinate and troposphere products, which are supplemented with variant rationales.

Within the processing, we screened station coordinate repeatabilities from weekly combined solutions and we identified any problematic station for which north/east/up residuals exceeded 15/15/30 mm or RMS of north/east/up coordinate component exceeded values 10/10/20 mm. Such station was a priori excluded from the tropospheric product for the corresponding day. There were other standard control procedures within the processing when individual station could have been excluded, e.g. if a) less than 60% of GNSS data available, b) code or phase data revealed poor quality, c) station metadata

were found inconsistent with data file header information (receiver, antenna and dome names, antenna eccentricities) and, d) phase residuals were too large for all satellites in the processing period indicating a problem with station. Tropospheric parameters were estimated practically without constraints (sigma greater than 1 m) thus parameter formal errors reflect relative uncertainties of estimates. Large errors usually indicate lack of observations contributing to the parameter. During the tropospheric parameter evaluations, we applied filter for exceeding formal errors of estimated parameters (ZTD sigma greater than 3 mm, normal cases stay below 1 mm). In monthly statistics we also applied iterative procedure for excluding residuals exceeding ~~3-sigma of standard deviation~~ calculated from the compared differences (Györi and Dousa, 2016).

3 Ensuring ZTD continuity at midnights

When site tropospheric parameter time series generated from the 2nd EUREF reprocessing are applied to climate research, they should be free of artificial offsets in order to avoid misinterpretations (Bock et al., 2014). However, GNSS processing is commonly performed on a daily basis according to adopted standards for data and product dissemination. Thus far, EUREF analysis centres have provided independent daily solutions, although precise IGS products are combined and distributed on a weekly basis. Station coordinates are estimated on a daily basis and are later combined to form more stable weekly solutions. According to the EUREF analysis centre guidelines (http://www.epncb.oma.be/documentation/guidelines/guidelines_analysis_centres.pdf), weekly coordinates should be used to estimate tropospheric parameters on a daily basis, but there are no requirements with which to guarantee the continuity of tropospheric parameters at midnights. Additionally, there are also discontinuities on a weekly basis, as neither daily coordinates nor hourly tropospheric parameters are combined across midnights between corresponding adjacent GPS weeks.

The impact of the 3-day combination was previously studied when assessing the tropospheric parameters stemming from the 2nd IGS reprocessing campaign 2016 (Dousa et al. 2016) in the GOP-TropDB (Györi and Douša, 2016). Figure 2 shows the hourly statistics when comparing two global tropospheric products from the analysis centre CODE (Centre of Orbit Determination in Europe) which differ in applying 1-day or 3-day combination within the final solution (Dach et al., 2014). The statistics is based on comparing 2-hour ZTD estimates from both solutions during 2013 while 1-sigma uncertainties over all stations are displayed as y-errorbars. The increased impact of 3-day solution on the ZTD accuracy can be observed close to midnights and indicates a 1-sigma uncertainty over differences in ZTDs at daily boundary stemming from 1-day and 3-day solutions. Actual differences in ZTDs are could be even significantly larger reaching up to several millimetres or more as the middle values of low-resolution ZTD estimates (2-hour) could have been compared only, i.e. at 1:00 UTC and 23:00 UTC every day.

During the 1st GOP reprocessing, there was no way to guarantee tropospheric parameter continuity at midnight, as the troposphere was modelled by applying a piecewise constant model. In these cases, tropospheric parameters with a temporal resolution of one hour were reported in the middle of the hour, as was originally estimated. In the 2nd GOP reprocessing, using again hourly estimates, we applied a piecewise linear model for the tropospheric parameters. The parameter continuities at midnights were not guaranteed implicitly, but only by an explicit combination of parameters at daily boundaries. For the combination procedure we used three consecutive days while the tropospheric product stems from the middle day. The procedure is done again for three consecutive days shifted by one day. A

similar procedure, using the piecewise constant model, was applied for estimating weekly coordinates which aimed to minimize remaining effects in consistency at transition of GPS weeks (at Saturday midnight). The coordinates of the weekly solution corresponding to the middle day of a three-day combination were fixed for the tropospheric parameter estimates. In the last step, we transformed the piecewise linear model to the piecewise constant model expressed in the middle of each hourly interval (HR:30), which was saved in the TRO-SINEX format to support the EUREF combination procedure requiring such sampling. The original piecewise linear parameter model was thus lost and to retain this information in the official product in the TRO-SINEX format, we additionally stored values for full hours (HR:00). Figure 3 summarizes four plots displaying tropospheric solutions with discontinuities in the left panels (a), (c) and enforcing tropospheric continuities in the right panels (b, d). While the upper plots (a), (b) display the piecewise constant model, bottom plots (c), (d) indicates the solution representing the piecewise linear model. The GOP Repro1 implementation is thus represented by Figure 3(a) plot while the GOP Repro2 solution corresponds to Figure 3(d).

These theoretical concepts were practically tested using a limited data set in 1996 (Figure 3). The panels in Figure 3 follow the organization of the theoretical plots shown in Figure 3; corresponding formal errors are also plotted along with estimated ZTDs. Discontinuities are visible in the left-hand plots and are usually accompanied by increasing formal errors for parameters close to data interval boundaries. As expected, discontinuities disappear in the right-hand plots. Although the values between 23:30 and 00:30 on two adjacent days are not connected by a line in the top-right plot, continuity was enforced for midnight parameters anyway, as seen in the bottom-right plot. Formal errors also became smooth near day boundaries, thus characterizing the contribution of data from both days and demonstrating that the concept behaves as expected in its practical implementation.

4 Assessment of reprocessing solutions

GOP variants and reprocessing models were assessed by a number of criteria, including those of the internal evaluations of coordinates' repeatability, residuals at reference stations, and the external validation of ZTDs and tropospheric horizontal gradients with data from numerical weather model (NWM) reanalyses.

4.1 Reference frame and station coordinates

We used coordinate repeatability to assess the quality of models applied in GNSS analysis. To be as thorough as possible, we not only assessed all GOP Repro2 variants but also assessed two GOP Repro1 solutions in order to discern improvements within the new reanalyses. The two Repro1 solutions differed in their used reference frames and PCV models: IGS05 and IGS08.

Table 3 summarizes mean coordinate repeatability in the north, east and up components of all stations from their weekly combinations. All GOP Repro2 solution variants reached approximately 50% and 25% of the lower mean RMS of coordinate repeatability when compared to the GOP Repro1/IGS08 solution in its horizontal and vertical components, respectively. These values represent even greater improvements when compared to the GOP-Repro1/IGS05 solution. Comparing these two Repro1 solutions clearly demonstrates the beneficial impact of the new PCV models and reference frames. The observed differences between Repro2 and Repro1 also indicate an overall improvement of the processing software from V5.0 to V5.2, and the enhanced quality of global precise orbit and earth orientation products.

Various GOP Repro2 solutions were also used to assess the selected models. Variants GO0 and GO1 differ in their mapping functions (GMF vs VMF1) used to project ZTDs into slant path delays. These comparisons demonstrate that vertical component repeatability improved from 4.14 mm to 3.97 mm, whereas horizontal component repeatability decreased slightly. By increasing the elevation angle cut-off from 3° to 7° (GO2) and 10° (GO3), we observed a slight increase in RMS from repeatabilities of all coordinates. This can be explained by the positive impact of low-elevation observations on the decorrelation of height and tropospheric parameters, despite the fact that applied models (such as elevation-dependent weighting, PCVs, multipath) are still not optimal for including observations at very low elevation angles. On the other hand, it should be noted that the VMF1 mapping function is particularly tuned to 3-degree elevations which leads to systematic errors at higher elevation angles, Zus et al. (2015).

The GO4 solution represents an official GOP contribution to EUREF combined products. It is identical to the variant GO1, but applies a non-tidal atmospheric loading. Steigenberger et al. (2009) discussed the importance of applying non-tidal atmospheric loading corrections together with precise a priori ZHD model. Using mean, or slowly varying, empirical pressure values for estimating a priori ZHD instead of true pressure values results in a partial compensation of atmospheric loading effects which is the case of GO1 solution. For GO4 solution we observed a ~~positive~~ improvement of approximately 9% for all coordinate components, which is less than the value of 20% previously observed on a global scale (Dach et al., 2011).



No impact was observed on higher-order ionospheric effects (GO4 vs. GO5) from this coordinate repeatability, as the effects are systematic within the regional network (Fritsche et al., 2005), and were thus mostly eliminated by using reference stations in the domains of interest. The combination of tropospheric horizontal gradients with 6- to 24-hour resolution (GO4 vs. GO6) with the piece-wise linear model was also discovered to have a negligible impact on the coordinates' repeatability.

The terrestrial reference frame (Altamimi et al., 2001) is a realization of a geocentric system of coordinates used by space geodetic techniques. To avoid a degradation of GNSS products, differential GNSS analysis methods require a proper referencing of the solution to the system applied in the generation of precise GNSS orbit products. For this purpose we often use the concept of fiducial stations with precise coordinates well-known in the requested system. Such stations are used to define the geodetic datum while their actual position can be re-adjusted by applying a condition minimizing coordinate residuals. None unique station is able to guarantee a stable monumentation and unchanged instrumentation during the whole reprocessing period. Thus a set of about 50 stations, with 100 and more time periods for reference coordinates, was carefully prepared for datum definition in the GOP reprocessing. An iterative procedure was applied for every day by comparing a priori reference coordinates with actually estimated ones and excluding fiducial station exceeding differences by 5, 5 and 15 mm in north, east and up components. Figure 5 shows the evolution of the number of actually used fiducial stations (represented as red dots) from all configured fiducial sites (represented as black dots) after applying an iterative procedure of validation on a daily basis. This reprocessing began with the use of 16-20 fiducial stations in 1996, and this number increased to reach a maximum of over 50 during the period from 2003-2011. After 2011, this number decreased, due to a common loss of reference stations available from the last realization of the global terrestrial reference frame without changes in its instrumentation. In most cases, only 2 or 3 stations were excluded from the total number, however, this number is lower for some daily solutions, indicating

the removal of even more stations. The lowest number of fiducial sites (12) was identified on day 209 of the year 1999 while, generally, low numbers were observed at the beginning of 1996. Generally, we observed consistent mean RMS errors for horizontal, vertical, and total residuals of 6.47, 10.22, and 12.25 mm and 4.83, 7.94, 9.35 mm for daily and weekly solutions, respectively, which demonstrate the stability of the reference system in the reprocessing. The seasonality in height coordinate estimates characterized by the RMS of residuals from the reference frame realization is dominated by errors due to modelling tropospheric parameters, and particularly wet contribution, during the different seasons as it will be clear also in the next section.

4.2 Zenith total delays

We compared all reprocessed tropospheric parameters with respect to independent data from the ERA-Interim global reanalysis (Dee et al. 2011), which were developed and provided by the European Centre for Medium-Range Weather Forecasts (ECMWF) from 1969 to the present. For the period of 1996-2014, we calculated tropospheric parameters (namely ZTD and tropospheric horizontal linear gradients) from the NWM for all EPN stations using the GFZ (German Research Centre for Geosciences) ray-tracing software (Zus et al., 2014).

Besides ZTDs, Table 4 also summarizes comparisons of the tropospheric horizontal delays with those obtained from the ERA-Interim. It indicates a mean ZTD bias -1.8 mm for all comparisons (GNSS – NWM) which seems to be related to the ERA-Interim suggesting underestimates of the water vapour content. Similar bias has been observed for all other European GNSS re-processing products (Pacione et al., 2017). Alternatively, the bias could be attributed to the ~~numerical weather data processing method~~. However, by processing ERA-Interim with two different software and methodologies within the GNSS4SWEC Benchmark campaign (Dousa et al., 2016) and by comparing them to two GNSS reference products based on different processing methods, we observed differences in bias below ± 0.4 mm. On the other hand, no systematic errors were identified in the Benchmark campaign between ERA-Interim and two GNSS reference ZTD solutions when using a small dense network in Central Europe and a short period in May-June 2013. Large negative bias (-4.9 mm) was, however, observed for ZTD parameters derived from the NCEP's Global Forecasting System when compared to the same reference GNSS reference ZTD solutions.

Comparing the results of the official GOP Repro2 solution (GO4) to those of the legacy solution (GO0) demonstrates an overall improvement of 9%, which corresponds to a similar comparison between the EUREF Repro1 and Repro2 products (Pacione et al., 2017). The improvement is assumed to be even larger (indicated by the coordinate repeatability), as the quality of ZTD retrievals are generally lower for NWM compared to GNSS from various intra-/inter-technique comparisons (Douša et al., 2016, Kačmařík et al., 2017, Bock and Nuret, 2009).

Comparing the GO1 and GO0 variants demonstrates that the VMF1 mapping function outperforms GMF in terms of standard deviations if a low elevation angle of 3 degrees is used. The change of mapping function together with the use of more accurate a priori ZHD, resulted in the ZTD standard deviation improving from 8.8 mm (GO0) to 8.3 mm (GO1). However, bias was slightly increased which could be partly attributed to the use of mean pressure model used for a priori ZTD calculation which is able to compensate part of the non-tidal atmospheric loading (see Section 4.1). Using non-tidal atmospheric loading corrections along with precise modelling of a priori ZHD contributed to a small reduction of the bias from -2.0 mm to -1.8 mm and, mainly, to the improvement by reducing this ZTD



accuracy to 8.1 mm (GO4), which corresponds with the previous assessment of the coordinates' repeatability. Degradation in ZTD precision was also observed when the elevation angle cut-off was raised from 3 degrees to 7 degrees (GO2) or 10 degrees (GO3). No impacts on ZTD were, however, visible neither from additional modelling of high-order ionospheric effects (GO5) nor from stacking of 6-hour horizontal gradients into daily estimates (GO6).

Figure 6 displays the time series of statistics from comparisons of the GOP official ZTD product (GO4) with respect to the results of the ERA-Interim reanalysis. Mean bias and standard deviation were derived from the monthly statistics of the 6-hourly GNSS-ERA differences. Standard errors of these mean values, represented by error bars, are additionally derived from all stations on a monthly basis. Although the time series show homogeneous results over the given time span, a small increase in the mean standard deviation over time likely corresponds with increasing number and more variable quality of EPN sites, rising from approximately 30 to 300. The early years (1996-2001) also display a worse overall agreement in standard errors of mean values, which can be attributed to the varying quality of historical observations and precise orbit products. The mean bias varies from -3 to 1 mm during the period of 1996-2014, with a long-term mean of -1.8 mm (Table 4). The long-term mean is also relatively small compared to the recorded ZTD mean uncertainty of about 3-5 mm.

4.3 Tropospheric horizontal linear gradients

Additional GNSS signal delay due to the tropospheric gradients were developed by McMillan (1995). The complete tropospheric model for the line-of-sight delay (ΔD_T) using parameters zenith hydrostatic delay (ZHD), zenith wet delay (ZWD) and first-order horizontal tropospheric gradients G_N and G_E , all expressed in units of length, is described as follows

$$\Delta D_T = mf_h(e)ZHD + mf_w(e)ZWD + mf_g(e)\cot(e)[G_N \cos(A) + G_E \sin(A)] \quad (1)$$

where e and a are observation elevation and azimuth angles and mf_h , mf_w , mf_g are hydrostatic, wet and gradient mapping functions representing the projection from an elevation to the zenith. Horizontal gradients should optimally represent a ZTD change in a distances for north and east directions as it could be represented by terms $G_N \cot(e)$ and $G_E \cot(e)$ in the equation. However, the gradients need to be parametrized practically with respect to observation elevation angle instead of the distance applicable theoretically to the tropospheric effect at various elevation angles. The interpretation of the tropospheric horizontal gradients in the Bernese software represents north and east components of angle applied for the tilting the zenith direction in the mapping function with gradients representing (in unit of length) the tilting angle multiplied by the delay in zenith (Meindl et al., 2004).

Figure 7 displays monthly time series of statistics from comparisons of the GNSS and NWM tropospheric horizontal gradients in north and east directions. Two solutions are highlighted in order to demonstrate the impact of different parameter temporal resolutions; a 6-hour resolution is used for GO4 and a 24-hour resolution is used for GO6. Seasonal variations are mainly pronounced when observing mean standard deviations (top plot), whereas gradual improvement is more pronounced for mean biases (bottom plot). The reduction of the initial mean biases and overall uncertainties in horizontal gradients are attributed to the improved availability and quality of low elevation observation tracking. Observation cut-off angle was configured individually at EPN stations from 0 to 15 degrees until 2008 when the cut-off angle 0 degrees was recommended for all the stations.

Mean standard deviations and their uncertainties (top plot of the figure) are lower by a factor of 1.3 for the solution with 24-hour resolution (GO6) compared to the 6-hour resolution (GO4); the impact is also pronounced especially in the early years of the dataset. The improvement factor ranges from 1.03 to 1.65 with the mean value of 1.35 overall stations and it is usually higher for years before 2001. Theoretically, with 4 times more observations in GO6 the standard deviation was expected to be divided by a factor of 2. This discrepancy indicates ~~serious~~ correlations in errors which are among others stemming from the errors in precise products and models. Significant improvements, however, indicates possible correlations between tropospheric gradients and other estimated parameters, such as ambiguities, height and zenith total delays, and suggests a careful handling particularly when applying a sub-daily temporal resolution.

As in case of ZTD and coordinate assessment, tropospheric gradients also recorded the degradation when raising the elevation angle cut-off from 3 degrees to 7 degrees (GO2) or 10 degrees (GO3) and no impact was observed from additional modelling of high-order ionospheric effects (GO5), see Table 4. Mean standard deviations of the GO2 and GO3 solutions increased by 8% and 12%, respectively, which was visible over the whole period in monthly time series (not ~~showed~~). No significant differences in temporal variations of mean biases of the north and east tropospheric gradients variants were identified while they shared a higher variability during the years 1996-2001.

Finally, comparing GO4 and GO6 solutions with ERA-Interim revealed that standard deviations dropped from 0.38 mm to 0.28 mm and from 0.40 mm to 0.29 mm for the east and north gradients, respectively. Worse performance of the GO4 solution is attributed to the fact that tropospheric horizontal gradients were estimated with a 6-hour sampling interval and a piece-wise linear function without the application of absolute or relative constraints. In such cases, increased correlations of these gradients with other parameters can cause additional instabilities in processing certain stations at specific times; these gradients can then absorb remaining errors in the GNSS analysis model. The mean biases of the tropospheric gradients are considered to be negligible, but we will demonstrate in the following section that some large systematic effects were indeed discovered and were attributed to the quality of GNSS signal tracking.

4.4 Spatial and temporal ZTD analysis

We performed spatial and temporal analyses of all processed variants in order to assess the impact of different settings on tropospheric products. Zenith tropospheric delays from all variants were compared in such a way to enable assessing impact of any single processing change: 1) GO1-GO0 for mapping function and more precise a priori ZHD model, 2) GO2-GO1 and GO3-GO1 for different elevation angle cut-off, 3) GO4-GO1 for non-tidal atmospheric corrections, 4) GO5-GO4 for higher-order ionospheric corrections and, 5) GO6-GO4 for temporal resolution tropospheric horizontal gradients. Station-specific behavior ~~is out of this paper and~~ will be studied in future.

Geographical maps of spatially distributed biases and standard deviations in ZTDs from all compared variants for the whole network are available within the supplementary materials. In the paper, we display only site-specific ZTD statistics with respect to the station ellipsoidal height, latitude and time in Figure 8, Figure 9 and Figure 10, respectively. Median, minimum and maximum values of station-wise total statistics are given in Table 5 ~~demonstrating the impact of the higher-order effect is negligible as well as mean biases, but for the GO1-GO0 comparison. Generally, height dependences are supposed to be mainly due to higher magnitudes of ZTDs increasing the impact of individual models~~

~~and their uncertainties. The impact on standard deviations is dominant in the GO1 vs. GO0 comparison, while impacts on systematic errors are visible more or less in all comparisons, Figure 8.~~

Using actual mapping function and precise a priori ZHD from VMF1 instead of blind GMF/GPT models (GO1 vs. GO0), we observe negative systematic errors ranging from -1.52 to 0.70 mm and the median value -0.36 mm, according to Table 5, with a moderate latitudinal dependence, see Figure 9. ~~A similar, but slightly larger negative bias of -0.94 ± 0.28 mm was reported Kacmarik et al. (2017) studying 400 stations in the central Europe.~~ Standard deviations in the table range from 0.69 mm to 3.82 mm, with a profound increase with latitude in Figure 9 suggesting the blind models perform worse at high latitudes. However, it is difficult to judge about the reason as it might be a product of mixed impact of a priori ZTD modelling, separating hydrostatic and wet component and applying mapping function. It suggests a more detailed study in future. Additionally, Figure 10 shows the effect grows with time which is attributed to the presence of more low-elevation observations as the elevation cut-off was updated gradually up to the horizon within the EUREF permanent network.

The impact of different elevation angle cut-off doesn't reveal any systematics in Figure 9. Biases for comparison of variants 3°/7° (GO2-GO1) and 3°/10° (GO3-GO1) range from -0.81 mm to 1.66 mm and -2.22 mm to 2.66 mm, respectively, and for standard deviations from 0.15 mm to 1.29 mm and 0.31 to 2.04 mm, see Table 5. As expected, the impact is larger for the GO3-GO1 differences and affected particularly some stations. Yearly biases exceeding ± 2.5 mm were identified for BELL, DENT, MLVL, MOPS, POLV RAMO and SBG2 EPN stations (<http://epncb.oma.be>). Temporal dependences in the GO2-GO1 and GO3-GO1 comparisons, see Figure 10, show systematic errors growing together with increasing impact of low-elevation observations in time.

The impact of non-tidal atmospheric loading (GO4-GO1) seems to be strongly site-specific and doesn't reveal any latitudinal dependence in Figure 9. It however shows some degradation prior the year 2002, see Figure 10, which hasn't been understood yet. Biases and standard deviations in Table 5 range from -2.29 mm to 5.55 mm and from 0.68 mm to 4.72 mm, respectively. It represents one the largest impact in term of systematic errors and the second largest impact in term of standard deviations when compared to other comparison variants. Generally, the effect corresponds to the site-specific modelling of non-tidal atmospheric loading corrections and their partial compensations via blind pressure model (GPT) used at GO0 for individual stations. Standard deviations above 3 mm were observed at these stations: JOZE, MAD2, MADR, MDVO, MOPI, NYAL, SBG2, VENE and WETT.

The impact of higher-order ionospheric effect (GO5-GO4) is negligible at all stations demonstrating total statistics for all stations within ± 0.3 mm with applying the y-range about 10 times smaller than in other panels in Figure 9. However, a strong latitudinal dependence is still visible in the figure and, a strong temporal variability shows yearly statistics up to ± 0.4 mm in Figure 10. Both dependences are due to the changing magnitude of ionospheric corrections, increasing towards equator, and due to the solar magnetic activity cycles, reaching peaks around years 2001 and 2014.

The impact of stacking tropospheric gradients from 6-hour to daily estimates (GO6-GO4) is almost negligible for systematic errors which stay below ± 1 mm. However, standard deviations range from 0.76 mm to 2.46 mm, growing towards lower latitudes, see Figure 9, which can be attributed to the increasing amount of water vapor content and its asymmetry imperfectly modelled by adding tropospheric gradients. Finally, there is no significant temporal variation observed in Figure 10.

5 Impact of variants on long-term trend estimates

We assessed the impact of processing variant settings on long-term trend estimates by analysing 12 EUREF stations providing the longest time-series of data. The trends were estimated using the least squares regression method applied on model

$$Y_t = \mu + \beta X_t + S_t + \varepsilon_t \quad (2)$$

where μ is the constant term of the model, βX_t is the linear trend function with β representing the trend magnitude, S_t represents the seasonal term modelled by the sine wave function of time X_t , including seasonal, sub-seasonal and high-frequencies, and finally ε_t is the noise in the data. Trend magnitudes were estimated using the original hourly ZTD estimates without any time-series homogenization, i.e. change-point detection and shift elimination. Data from all variants were processed for all selected stations and displayed in Figure 11. Trends ranged from -0.05 to 0.38 mm/year with formal errors of 0.01-0.02 mm/year. The most significant impact was observed due to the changing elevation angle cut-off reaching differences up to 1 mm/year in ZTD while the impact of any other strategy change was below 0.5 mm/year only.

6 Tropospheric gradients biases vs quality of observations

Using a new interactive web interface to conduct tropospheric parameter comparisons in the GOP-TropDB (Györi and Douša, 2016), we observed large systematic tropospheric gradients during specific years at several EPN stations. Generally, from GNSS data, we can only estimate total tropospheric horizontal gradients without being able to distinguish between dry and wet contributions. The former is mostly due to horizontal asymmetry in atmospheric pressure, and the latter is due to asymmetry in the water vapour content. The latter is thus more variable in time and space than the former (Li et al., 2015). Regardless, mean gradients should be close to zero, whereas dry gradients may tend to point slightly more to the equator, corresponding to latitudinal changes in atmosphere thickness (Meindl et al., 2004). Similarly, orography-triggered horizontal gradients can appear due to the presence of high mountain ranges in the vicinity of the station (Morel et al., 2015). Such systematic effects can reach the maximum sub-millimetre level, while a higher long-term gradient (i.e., >1 mm), is likely more indicative of issues with site instrumentation, the environment, or modelling effects. Therefore, in order to clearly identify these systematic effects, we also compared our gradients with those calculated from the ERA-Interim.

It is beyond the scope of this paper to investigate in detail the correlation between tropospheric horizontal gradients and antenna tracking performance. However, we do observe a strong impact in the most extreme case identified when comparing gradients from the GNSS and the ERA-Interim for all EPN stations. Figure 12 shows the monthly means of differences in the north and east tropospheric gradients from the MALL station (Mallorca, Spain). These differences increase from 0 mm up to -4 mm and 2 mm for the east and north gradients, respectively, within the period of 2003/06 - 2008/10. Such large monthly differences in GNSS and NWM gradients are not realistic, and were attributed to data processing when long-term increasing biases immediately dropped down to zero on November 1, 2008, immediately after the antenna and receiver were changed at the station. During the same period, the period, also yearly mean ZTD differences to ERA-Interim steadily changed from about 3 mm to about -12 mm and immediately dropping down to -2 mm in 2008 after the antenna change.

The EPN Central Bureau (<http://epncb.oma.be>), operating at the Royal Observatory of Belgium (ROB), provides a web service for monitoring GNSS data quality and includes monthly snapshots of the tracking characteristics of all stations. The sequence of plots displayed in Figure 13, representing the interval of interest (2002, 2004, 2006 and 2008), reveals a slow but systematic and horizontally asymmetric degradation of the capability of the antenna to track low-elevation observations at the station. Therefore, we analysed days of the year (DoY) 302 and 306 (corresponding to October 28 and November 1, 2008) with the in-house G-Nut/Anubis software (Václavovic and Douša, 2016) and observed differences in the sky plots of these two days. The left-hand plot of Figure 14 depicts the severe loss of dual-frequency observations up to a 25-degree elevation angle in the South-East direction (with an azimuth of 90-180 degrees), which cause the tropospheric linear gradient of approximately 5 mm to point in the opposite direction. Figure 10 also demonstrates that an increasing loss of second frequency observations appears to occur in the East (represented as black dots). The right-hand plot in this figure demonstrates that both of these effects fully disappeared after the antenna was replaced on October 30, 2008 (DoY 304), resulting in the appearance of normal sky plot characteristics and a GLONASS constellation with one satellite providing only single frequency observations (represented as black lines).

This situation demonstrates the high sensitivity of the estimated gradients on data asymmetry, particularly at low-elevation angles. The systematic behaviour of these monthly mean gradients, their variations from independent data, and their profound progress over time seem to be useful indicators of instrumentation-related issues at permanent GNSS stations. It is also considered that gradient parameters can be valuable method as a part of ZTD data screening procedure (Bock et al., 2016).

Although the station MALL represented an extreme case, biases at other stations were observed too, e.g. GOPE (1996-2002), TRAB (1999-2008), CREU (2000-2002), HERS (1999-2001), GAIA (2008-2014) and others. Site-specific, spatially or temporally correlated biases suggest different possible reasons such as site-instrumentation effects including the tracking quality and phase centre variation models, site-environment effects including multipath and seasonal variation (e.g. winter snow/ice coverage), edge-network effects when processing double-difference observations, spatially correlated effects in reference frame realization and possibly others. More detail investigation is out of the scope of this paper and will be studied in future.

7 Conclusions

In this paper, we present results of the new GOP reanalysis of all stations within the EUREF Permanent network during the period of 1996-2014. This reanalysis was completed during the 2nd EUREF reprocessing to support the realization of a new European terrestrial reference system. In the 2nd reprocessing, we focused on analysing a new product – GNSS tropospheric parameter time-series for applications to climate research. To achieve this goal, we improved our strategy for combining tropospheric parameters at midnights and at transitions in GPS weeks. We also performed seven solution variants to study optimal troposphere modelling; we assessed each of these variants in terms of their coordinate repeatability by using internal evaluations of the applied models and strategies. We also compared tropospheric ZTD and tropospheric horizontal gradients with independent evaluations obtained by numerical weather reanalysis via the ERA-Interim.

496 Results of the GOP Repro2 yielded improvements of approximately 50% and 25% for their horizontal
497 and vertical component repeatability, respectively, when compared to those of the GOP Repro1
498 solution. Vertical repeatability was reduced from 4.14 mm to 3.73 mm when using the VMF1 mapping
499 function, a priori ZHD, and non-tidal atmospheric loading corrections from actual weather data.
500 Increasing the elevation angle cut-off from 3° to 7°/10° increased RMS errors of residuals from these
501 coordinates' repeatability. All of these factors were also confirmed by the independent assessment of
502 tropospheric parameters using NWM reanalysis data.

503 We particularly recommend using low-elevation observations along with the VMF1 mapping function,
504 as well as using precise a priori ZHD values with the consistent model of non-tidal atmospheric loading.
505 While estimating tropospheric horizontal linear gradients improves coordinates' repeatability, 6-hour
506 sampling without any absolute or relative constraints revealed a loss of stability due to their
507 correlations with other parameters.

508 Assessing the tropospheric horizontal gradients with respect to the ERA-Interim reanalysis data
509 revealed some long-term systematic behaviour linked to degradation in antenna tracking quality. We
510 presented an extreme case at the Mallorca station (MALL), in which gradients systematically increased
511 up to 5 mm from 2003-2008 while pointing in the direction of prevailing observations at low elevation
512 angles. However, these biases disappeared when the malfunctioning antenna was replaced. More
513 cases similar to this, although less extreme, have indicated that estimated tropospheric gradients are
514 extremely sensitive to the quality of GNSS antenna tracking, thus suggesting that these gradients can
515 be used to identify problems with GNSS data tracking in historical archives.

516 The impact of processing variants on long-term ZTD trend estimates was assessed at 12 long-term
517 EUREF stations. The most significant impact was due to the changing elevation angle cut-off reaching
518 differences up to 1 mm/year in ZTD while impacts of other strategy changes stayed below 0.5
519 mm/year.

520 Finally, one of the main difficulties faced during the 2nd reprocessing was that of the quality of the
521 historical data, which contains a large variety of problems. We removed data that caused significant
522 problems in network processing when these could not be pre-eliminated from normal equations
523 during the combination process without still affecting daily solutions. To provide high-accuracy, high-
524 resolution GNSS tropospheric products, the elimination of such problematic data or stations is even
525 more critical considering the targeting static coordinates on a daily or weekly basis for the maintenance
526 of the reference frame or the derivation of a velocity field. Before undertaking the 3rd EUREF
527 reprocessing, which is expected to begin after significant improvements have been made to state-of-
528 the-art models, products and software, we need to improve data quality control and clean the EUREF
529 historical archive in order to optimize any future reprocessing efforts and to increase the quality of
530 tropospheric products. These efforts should also include the collection and documentation of all
531 available information from each step of the 2nd EUREF reprocessing, including individual contributions,
532 EUREF combinations, time-series analyses and coordinates, and independent evaluations of
533 tropospheric parameters.

Acknowledgments

The reprocessing effort and its evaluations were supported by the Ministry of Education, Youth and Science, the Czech Republic (projects LD14102 and LO1506). We thanks two anonymous reviewers and Dr. Olivier Bock for comments and suggestions which helped us to improve the manuscript.

References

- Altamimi, Z., Angermann, D., Argus, D., et al.: The terrestrial reference frame and the dynamic Earth, EOS, Transactions, American Geophysical Union, 82, 273–279, 2001.
- Bevis, M., Businger, S., Chiswell, S., Herring, T. A., Anthes, R. A., Rocken C, and Ware R. H.: GPS Meteorology: Mapping Zenith Wet Delays onto Precipitable Water, J. Appl. Meteorol., 33, 379–386, 1994.
- Bock, O., Willis, P., Wang, J., and Mears, C.: A high-quality, homogenized, global, long-term (1993–2008) DORIS precipitable water data set for climate monitoring and model verification, J. Geophys. Res. Atmosphere, 119, 7209–7230, 2014.
- Bock, O., and Nuret, M.: Verification of NWP model analyses and radiosonde humidity data with GPS precipitable water vapor estimates during AMMA, Weather and Forecasting, 24(4), 1085–1101, 2009.
- Bock, O., Bosser, P., Pacione, R., Nuret, M., Fourrié, N., and Parracho, A.: A high-quality reprocessed ground-based GPS dataset for atmospheric process studies, radiosonde and model evaluation, and reanalysis of HyMeX Special Observing Period. Q.J.R. Meteorol. Soc., 142, 56–71, 2016.
- Böhm, J., Niell, A. E., Tregoning, P., and Schuh, H.: 2006, Global Mapping Functions (GMF): A new empirical mapping function based on numerical weather model data, Geophys. Res. Lett., 33, L07304, 2006a.
- Böhm, J., Werl, B., and Schuh, H.: Troposphere mapping functions for GPS and very long baseline interferometry from European Centre for Medium-Range Weather Forecasts operational analysis data. J. Geophys. Res., 111, B02406, 2006b.
- Bruyninx, C., Habrich, H., Söhne, W., Kenyeres, A., Stangl, G., and Völksen, C.: Enhancement of the EUREF Permanent Network Services and Products, Geodesy for Planet Earth, IAG Symposia Series, 136, 27–35, 2012.
- Dach, R., Böhm, J., Lutz, S., Steigenberger, P., and Beutler, G.: Evaluation of the impact of atmospheric pressure loading modeling on GNSS data analysis, J. Geod., 85(2), 75–91, 2011.
- Dach, R., Schaer, S., Lutz, S., Baumann, C., Bock, H., Orliac, E., Prange, L., Thaller, D., Mervart, L., Jäggi, A., Beutler, G., Brockmann, E., Ineichen, D., Wiget, A., Weber, G., Habrich, H., Söhne, W., Ihde, J., Steigenberger, P., and Hugentobler, U.: CODE IGS Analysis Center Technical Report 2013, Dach, R., and Jean, Y. (eds.), IGS 2013 Tech. Rep., 21–34, 2014.
- Dach, R., Lutz, S., Walser, P., and Fridez, P. (Eds.): Bernese GNSS Software Version 5.2. User manual, Astronomical Institute, University of Bern, Bern Open Publishing, 2015.
- Dee, D.P., Uppala, S.M., Simmons, A.J. et al.: The ERA-Interim reanalysis: Configuration and performance of the data assimilation system, Q. J. Roy. Meteorol. Soc., 137, 553–597, 2011.
- Douša, J., and Václavovic, P.: Results of GPS Reprocessing campaign (1996–2011) provided by Geodetic observatory Pecný, Geoinformatics, FCE CTU, 9, 77–89, 2012.

- Douša, J., Dick, G., Kačmařík, M., Brožková, R., Zus, F., Brenot, H., Stoycheva, A., Möller, G., and Kaplon, J.: Benchmark campaign and case study episode in central Europe for development and assessment of advanced GNSS tropospheric models and products, *Atmos. Meas. Tech.*, 9, 2989–3008, 2016.
- Douša, J., Böhm, O., Byram, S., Hackman, C., Deng Z., Zus, F., Dach, R., and Steigenberger, P.: Evaluation of GNSS reprocessing tropospheric products using GOP-TropDB, IGS Workshop 2016, Sydney, February 8–12, 2017, available at: <http://www.igs.org/assets/pdf/W2016%20-%20PS0303%20-%20Dousa.pdf>
- Fritsche, M., Dietrich, R., Knofel, C., Rülke, A., Vey, S., Rothacher, M., and Steigenberger, P.: Impact of higher-order ionospheric terms on GPS estimates. *Geophys. Res. Lett.*, 32, L23311, 2005.
- Györi, G., and Douša, J.: GOP-TropDB developments for tropospheric product evaluation and monitoring – design, functionality and initial results, *IAG Symposia Series*, Springer, 143, 595–602, 2016.
- Ihde, J., Habrich, H., Sacher, M., Sohne, W., Altamimi, Z., Brockmann, E., Bruyninx, C., Caporali, A., Dousa, J., Fernandes, R., Hornik, H., Kenyeres, A., Lidberg, M., Makinen, J., Poutanen, M., Stangl, G., Torres, J.A., and Volksen, C.: EUREF's Contribution to National, European and Global Geodetic Infrastructures, In: *Earth on the Edge: Science for a Sustainable Planet*, Rizos, C. and Willis P. (eds), *IAG Symposia Series*, Springer, 139, 189–196, 2014.
- IERS Conventions: Gérard, P., and Luzum, B. (Eds.), *IERS Technical Note No. 36*, Frankfurt am Main: Verlag des Bundesamts für Kartographie und Geodäsie, 179 pp., 2010.
- Kačmařík, M., Douša, J., Dick, G., Zus, F., Brenot, H., Möller, G., Pottiaux, E., Kaplon, J., Hordyniec, P., Václavovic, P., and Morel, L.: Inter-technique validation of tropospheric slant total delays, Accepted for *Atmos. Meas. Tech.* 2017.
- Li, X., Zus, F., Lu, C., Ning, T., Dick, G., Ge, M., Wickert, J., and Schuh, H.: Retrieving high-resolution tropospheric gradients from multiconstellation GNSS observations, *Geophys. Res. Lett.*, 42(10), 4173–4181, 2015.
- Meindl, M., Schaer, S., Hugentobler, U., and Beutler, G.: Tropospheric Gradient Estimation at CODE: Results from Global Solutions. *Journal of the Meteorological Society of Japan*, 82, 331–338, 2004.
- Morel, L., Pottiaux, E., Durand, F., Fund, F., Follin, J.M., Durand, S., Bonifac, K., Oliveira, P.S., van Baelen, J., Montibert, C., Cavallo, T., Escaffit, R., and Fragnol, L.: Global validity and behaviour of tropospheric gradients estimated by GPS, presentation at the 2nd GNSS4SWEC Workshop held in Thessaloniki, Greece, May 11–14, 2015.
- MacMillan, D. S.: Atmospheric gradients from very long baseline interferometry observations, *Geophys. Res. Lett.*, 22, 1041–1044, 1995.
- Meindl, M., Schaer, S., Hugentobler, U., and Beutler, G.: Tropospheric Gradient Estimation at CODE: Results from Global Solutions. *J. Meteorol. Soc. Japan*, 82, 331–338, 2004.
- Ning, T.: GPS Meteorology: With Focus on Climate Applications, PhD Thesis, Dept. Earth and Space Sciences. Chalmers University of Technology, 2012.
- Pacione, R., Araszkiewicz, A., Brockmann, E., and Dousa, J.: EPN-Repro2: A reference GNSS tropospheric data set over Europe, *Atmos. Meas. Tech.*, 10, 1689–1705, doi:10.5194/amt-10-1689-2017, 2017.

- Steigenberger, P., Böhm, J., and Tesmer, V.: Comparison of GMF/GPT with VMF1/ECMWF and implications for atmospheric loading, *J. Geod.*, 83, 943, 2009.
- Václavovic, P., and Douša, J.: G-Nut/Anubis – open-source tool for multi-GNSS data monitoring, In: *IAG 150 Years*, Rizos, Ch. and Willis, P. (eds), *IAG Symposia Series*, Springer, 143, 775–782, 2016.
- Völksen, C.: An update on the EPN Reprocessing Project: Current Achievements and Status, Presented at the EUREF 2011 Symposium, Chisinau, Republic of Moldova, May 25–28. http://www.epncb.oma.be/_documentation/papers/eurefsymposium2011/an_update_on_e_pn_reprocessing_project_current_achievement_and_status, 2011
- Yuan, L.L., Anthes, R.A., Ware, R.H., Rocken, C., Bonner, W.D., Bevis, M.G., and Businger, S.: Sensing Climate Change Using the Global Positioning System, *J. Geophys. Res.*, 98, 14925–14937, 1993.
- Zus, F., Dick, G., Heise, S., Dousa, J., and Wickert, J.: The rapid and precise computation of GPS slant total delays and mapping factors utilizing a numerical weather model, *Radio Sci.*, 49, 207–216, 2014.
- Zus, F., Dick, G., Dousa, J., and Wickert, J.: Systematic errors of mapping functions which are based on the VMF1 concept, *GPS Solut.*, 19(2), 277–286, 2015.

636 **Table 1: Characteristics of GOP reprocessing models**

Processing options	Description
Products	CODE precise orbit and earth rotation parameters from the 2 nd reprocessing.
Observations	Dual-frequency code and phase GPS observations from L1 and L2 carriers. Elevation cut-off angle 3 degree, elevation-dependent weighting $1/\cos^2$ (zenith), double-difference observations and with 3-minute sampling rate.
Reference frame	IGb08 realization, core stations set as fiducial after a consistency checking. Coordinates estimated using a minimum constraint.
Antenna model	GOP: IGS08_1832 model (receiver and satellite phase centre offsets and variations).
Troposphere	A priori zenith hydrostatic delay/mapping function: GPT/GMFh (GO0) and VMF1/VMF1h (GO1-GO6). Estimated ZWD corrections every hour using VMF1 wet mapping function; 5 m and 1 m for absolute and relative constraints, respectively. Estimated horizontal NS and EW tropospheric gradients every 6 hours (GO0-GO5) or 24 hours (GO6) without a priori tropospheric gradients and constraints.
Ionosphere	Eliminated using ionosphere-free linear combination (GO0-GO6). Applying higher-order effects estimated using CODE global ionosphere product (GO5).
Loading effects	Atmospheric tidal loading and hydrology loading not applied. Ocean tidal loading FES2004 used. Non-tidal atmospheric loading introduced in advanced variants from the model from TU-Vienna (GO4-GO6).

637

638 **Table 2: GOP solution variants for the assessment of selected models and settings**

Solution ID	Specific settings and differences	Remarks and rationales
G00	GMF and 3° cut-off	Legacy solution for Repro1
G01	VMF1 and 3° cut-off	New candidate for Repro2
G02	=G01; 7° cut-off	Impact of elevation degree cut-off
G03	=G01; 10° cut-off	Impact of elevation degree cut-off
G04	=G01; atmospheric loading	Non-tidal atmospheric loading applied
G05	=G04; higher-order ionosphere	Higher-order ionosphere effect not applied
G06	=G04; 24-hour gradients	Stacking tropospheric gradients to 24-hour sampling

639

640

Table 3: Comparison of GOP solution variants for north, east and up coordinate repeatability.

Solution	North RMS [mm]	East RMS [mm]	Up RMS [mm]
GOP-Repro1/IGS05	3.01	2.40	5.08
GOP-Repro1/IGS08	2.64	2.21	4.94
GO0	1.20	1.30	4.14
GO1	1.23	1.33	3.97
GO2	1.24	1.33	4.01
GO3	1.26	1.34	4.07
GO4	1.14	1.24	3.73
GO5	1.14	1.24	3.73
GO6	1.14	1.24	3.73

641

642 **Table 4: Statistics (bias and standard deviations) of ZTD and tropospheric gradients from the seven reprocessing variants**
643 **compared to those obtained from the ERA-Interim NWM reanalysis.**

Solution	ZTD bias [mm]	ZTD sdev [mm]	EGRD bias [mm]	EGRD sdev [mm]	NGRD bias [mm]	NGRD sdev [mm]
GO0	-1.5 ± 2.1	8.8 ± 2.0	-0.04 ± 0.08	0.39 ± 0.10	+0.01 ± 0.09	0.43 ± 0.12
GO1	-2.0 ± 2.1	8.3 ± 2.2	-0.04 ± 0.08	0.39 ± 0.10	+0.01 ± 0.09	0.43 ± 0.13
GO2	-1.9 ± 2.2	8.4 ± 2.2	-0.05 ± 0.10	0.41 ± 0.10	+0.00 ± 0.12	0.43 ± 0.12
GO3	-1.8 ± 2.3	8.5 ± 2.1	-0.08 ± 0.13	0.43 ± 0.11	-0.01 ± 0.14	0.43 ± 0.12
GO4	-1.8 ± 2.4	8.1 ± 2.1	-0.04 ± 0.09	0.38 ± 0.10	+0.00 ± 0.09	0.43 ± 0.12
GO5	-1.8 ± 2.4	8.1 ± 2.1	-0.05 ± 0.09	0.38 ± 0.10	+0.01 ± 0.08	0.43 ± 0.12
GO6	-1.8 ± 2.4	8.2 ± 2.1	-0.04 ± 0.08	0.29 ± 0.06	+0.01 ± 0.09	0.43 ± 0.06

644

645 **Table 5: Median, minimum (min) and maximum (max) values of total ZTD biases and standard deviation (sdev) over all**
646 **stations. Units are millimetres.**

Compared variants	ZTD bias median	ZTD bias min	ZTD bias max	ZTD sdev median	ZTD sdev min	ZTD sdev max
GO1-GO0	-0.36	-1.52	+0.70	2.01	0.69	3.82
GO2-GO1	+0.03	-0.81	+1.66	0.66	0.15	1.29
GO3-GO1	+0.03	-2.22	+2.66	1.10	0.31	2.04
GO4-GO1	+0.05	-3.29	+5.55	1.37	0.68	4.72
GO5-GO4	-0.02	-0.31	+0.07	0.07	0.04	0.30
GO6-GO4	-0.02	-0.23	+0.16	1.24	0.76	2.46

647

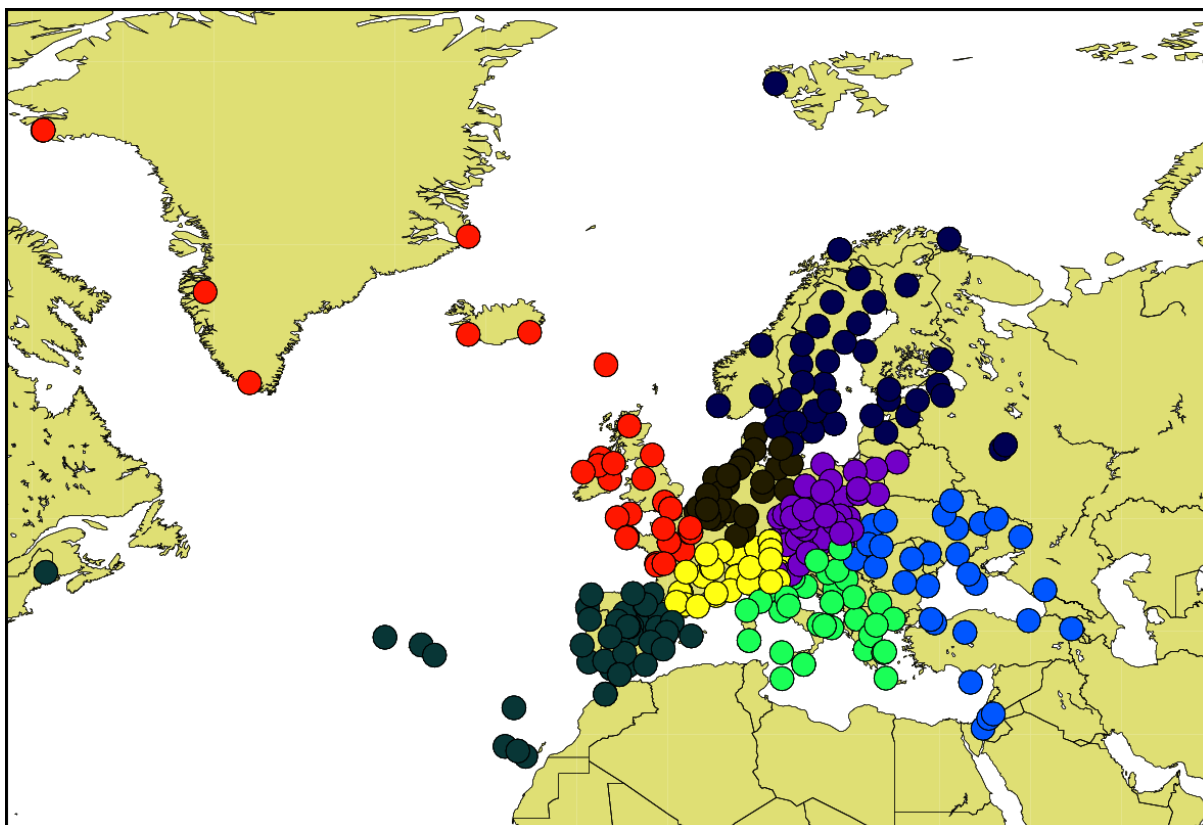


Figure 1: EUREF Permanent Network's clusters (designated by different colours) in the 2nd GOP reprocessing.

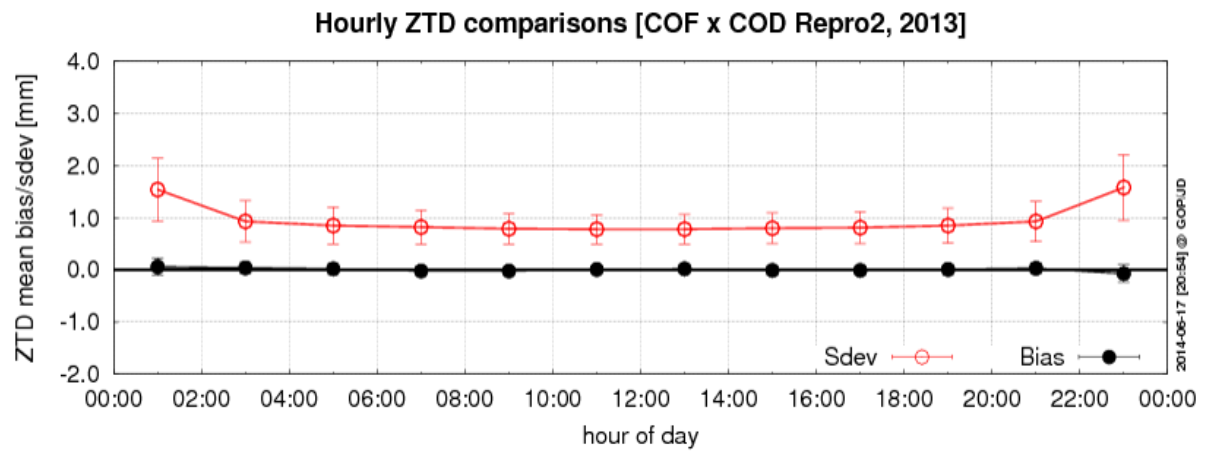
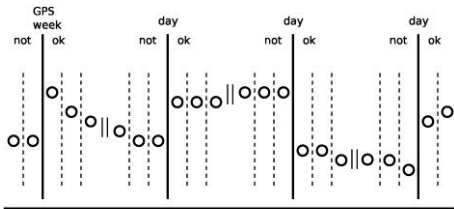
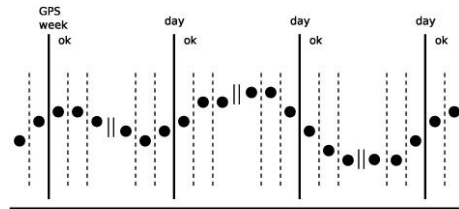


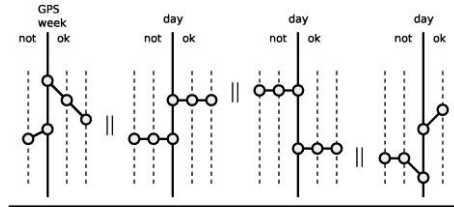
Figure 2: Hourly comparison of ZTDs (in 2013) from two CODE global 2nd IGS reprocessing products using 1-day (COF) and 3-day (COD) solutions. Error bars indicate standard errors of mean values over all compared stations.



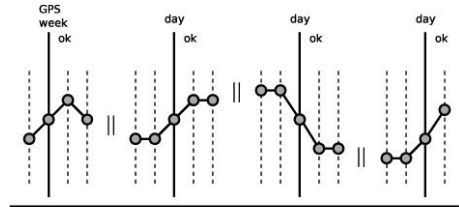
(a) time ->



(b) time ->



(c) time ->



(d) time ->

Figure 3: Charts of 4 variations on representations of tropospheric parameters. Right (b), (d) and left (a), (c) panels display estimates made with and without midnight combinations, respectively. Top (a), (b) and bottom (c), (d) panels display the piecewise constant and the linear model, respectively.

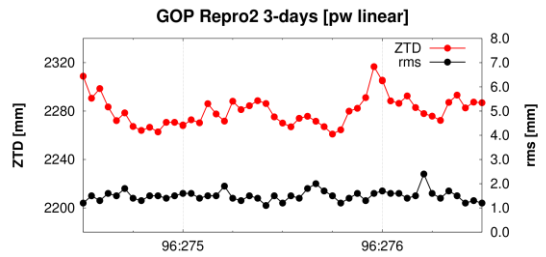
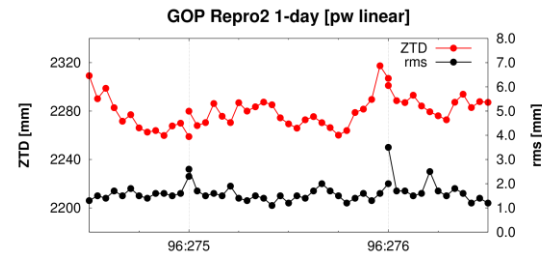
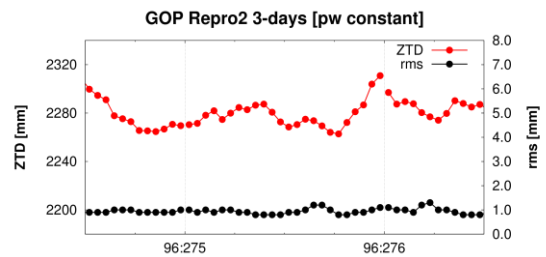
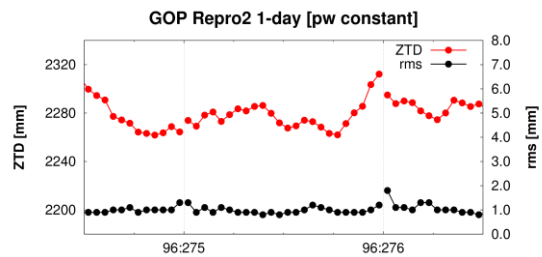


Figure 4: Four variations in representation of tropospheric parameters. Right (b), (d) and left (a), (c) panels display estimates with and without midnight combinations, respectively. Top (a), (b) and bottom (c), (d) panels display the piecewise constant and the piecewise linear model, respectively.

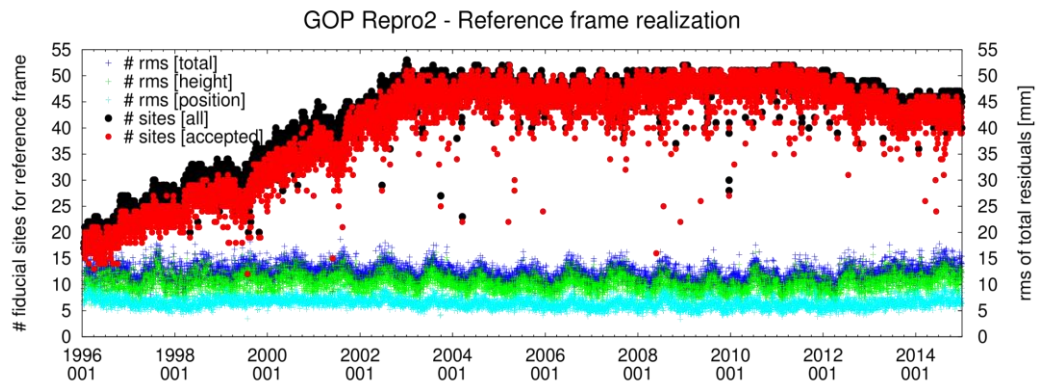


Figure 5: Statistics of the daily reference system realization: a) RMS of residuals at fiducial stations (representing the total, height and position); b) number of stations (all and accepted after an iterative control)

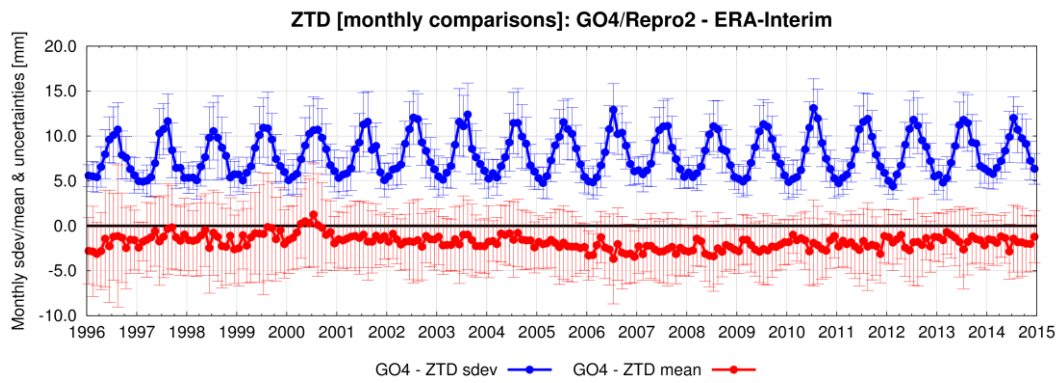


Figure 6: Monthly means of bias and standard deviation of official GOP ZTD product compared to those of the ERA-Interim. Error bars indicate standard errors of mean values over all compared stations.

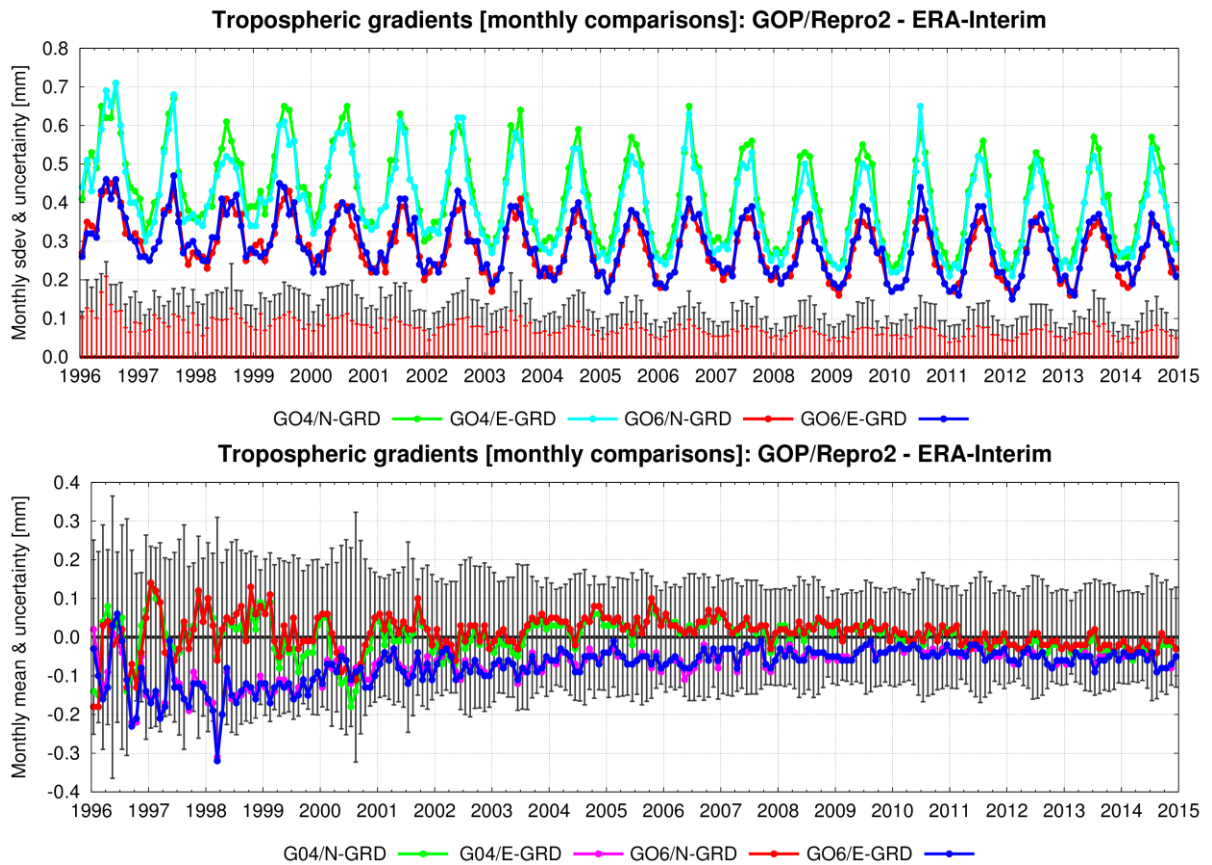


Figure 7: Monthly means of bias and standard deviation of tropospheric horizontal north (N-GRD) and east (E-GRD) gradients compared to those obtained by ERA-Interim. Note: Similar products are almost superposed. Error bars indicate standard errors of mean values over all compared stations plotted from the zero y-axis to emphasise seasonal variations and trends. Error bars are displayed for north gradients only, however, being representative for the east gradients too.

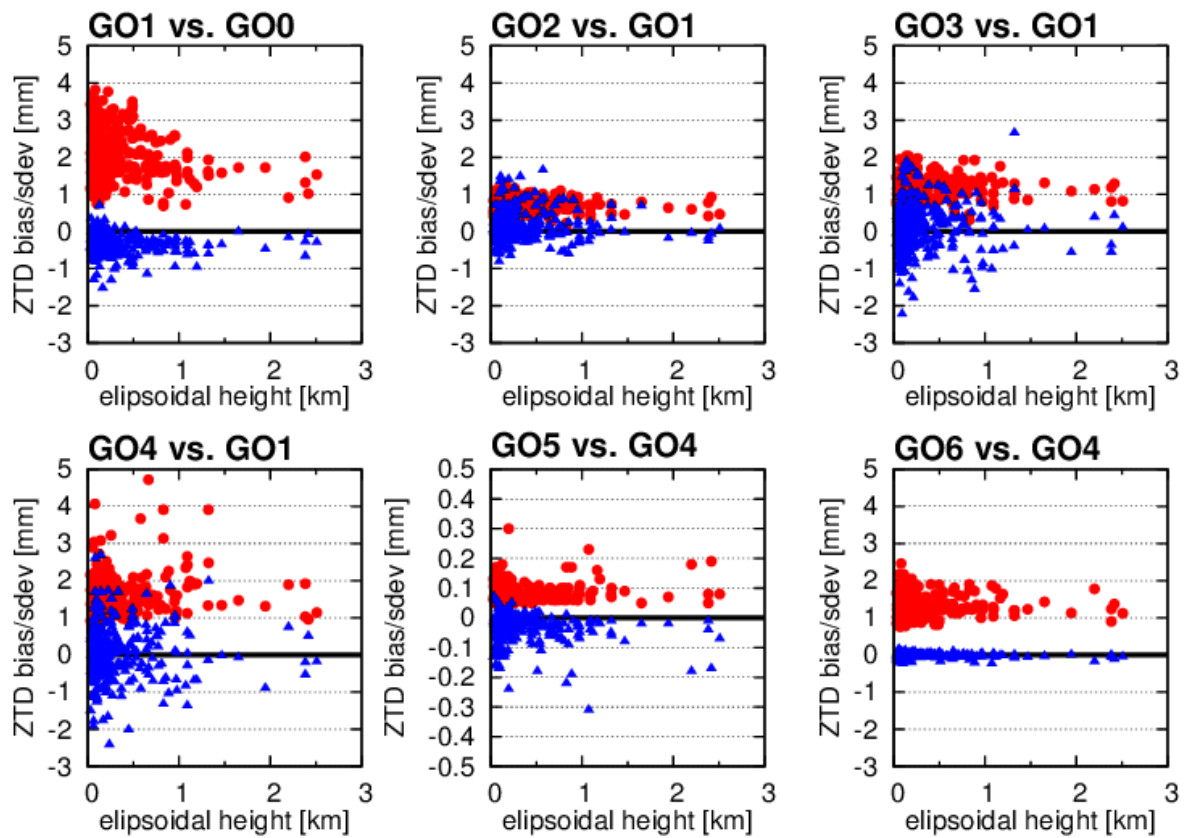


Figure 8: Dependence of ZTD systematic errors (blue) and standard deviations (red) from inter-comparisons of GOP 2nd reprocessing solution variants on station ellipsoidal height. Note different y-range for the GO5 vs. GO4 comparison.

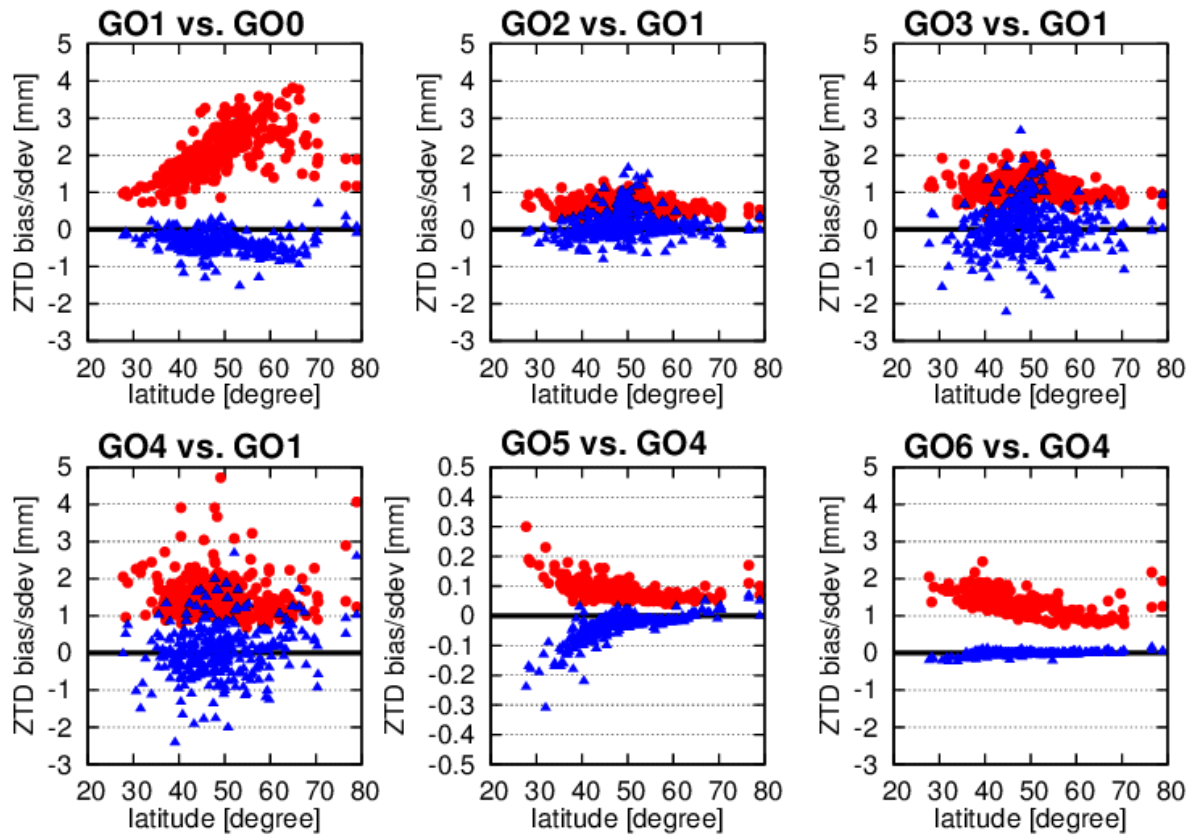


Figure 9: Dependence of ZTD systematic errors (blue) and standard deviations (red) from inter-comparisons of GOP 2nd reprocessing solution variants on station latitude. Note different y-range for the GO5 vs. GO4 comparison.

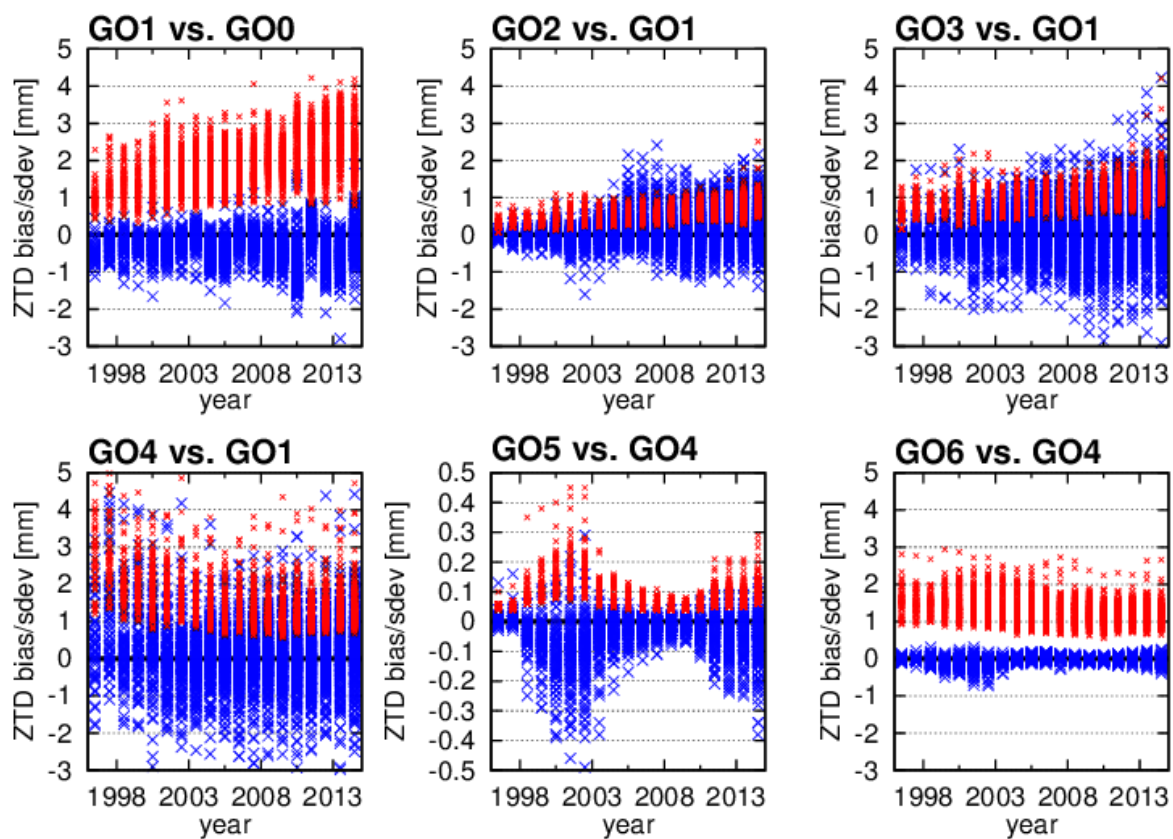


Figure 10: Dependence of ZTD systematic errors (blue) and standard deviations (red) from inter-comparisons of GOP 2nd reprocessing solution variants on year. Note different y-range for the GO5 vs. GO4 comparison.

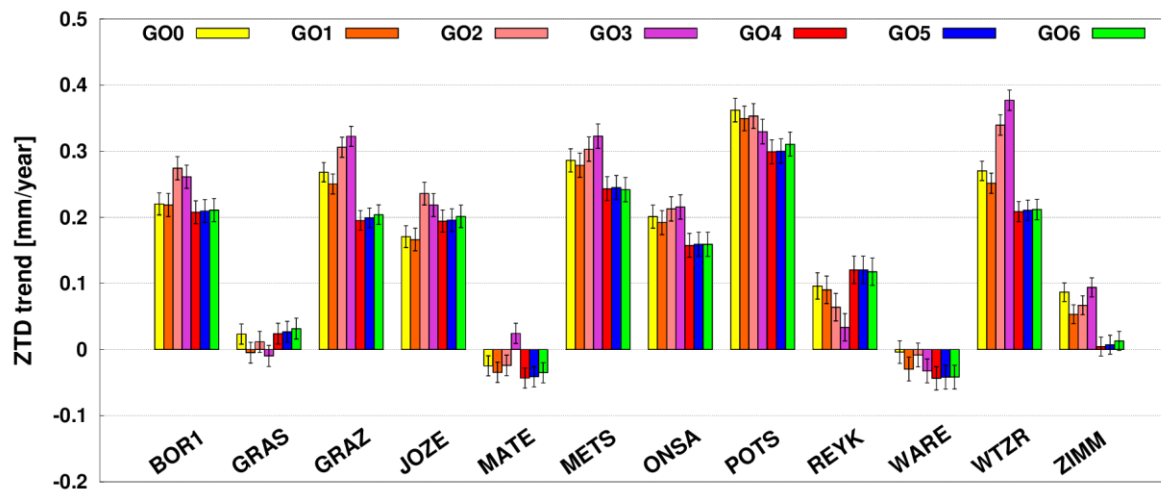


Figure 11: Long-term ZTD trend estimates and their formal errors (error bars) for all processing variants.

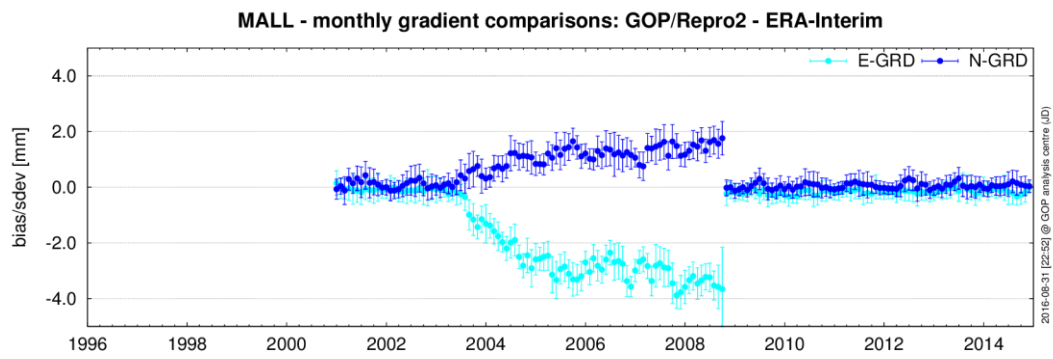


Figure 12: MALL station - monthly mean differences in tropospheric horizontal gradients with respect to the ERA-Interim.

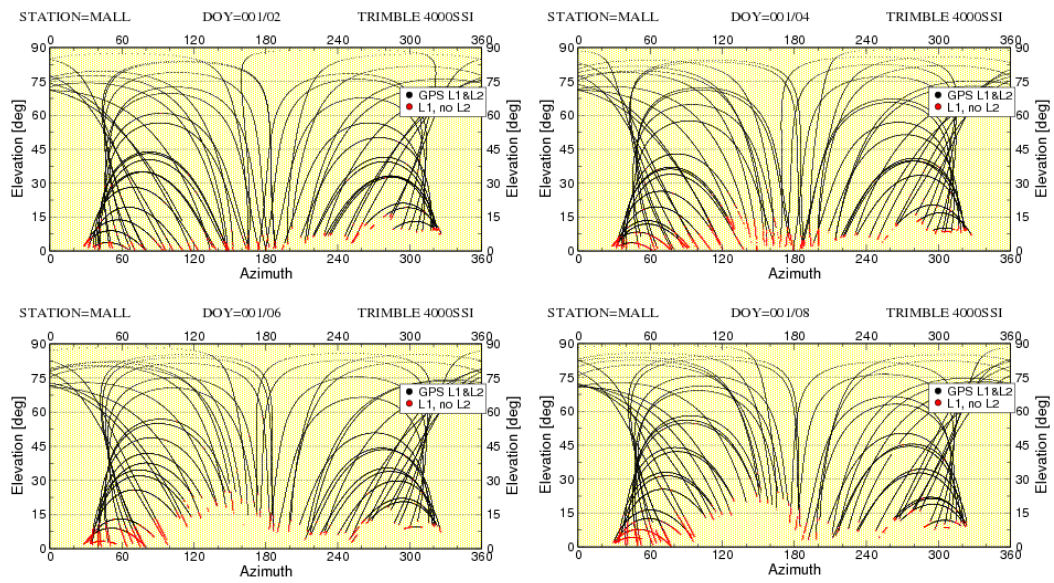


Figure 13: Low-elevation tracking problems at the MALL station during the period of 2003-2008. From left-top to right-bottom: January 2002, 2004, 2006 and 2008 (courtesy of the EPN Central Bureau, ROB).

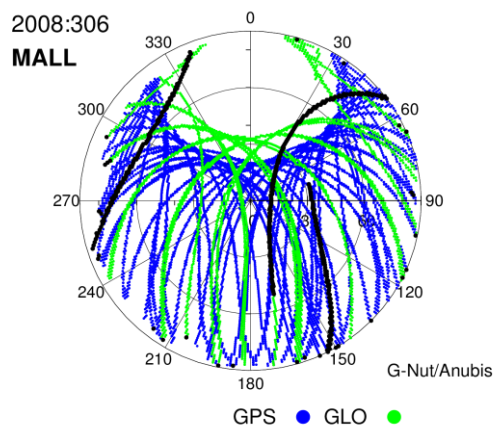
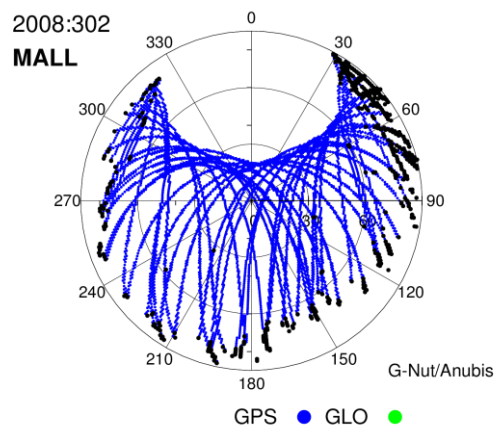


Figure 14: Sky plots before (left) and after (right) replacing the malfunctioning antenna at the MALL site (Oct 30, 2008).
Black dots indicates single-frequency observations available only.